Mechanisms of Chloride Interferences in Atomic Absorption Spectrometry Using a Graphite Furnace Atomizer Investigated by Electrothermal Vaporization Inductively Coupled Plasma Mass Spectrometry

Part 1. Effect of Magnesium Chloride Matrix and Ascorbic Acid Chemical Modifier on Manganese*

J. P. Byrne
Department of Chemistry, University of Technology, Sydney, P.O. Box 123, Broadway, New South Wales 2007, Australia

C. L. Chakrabarti†
Centre for Analytical and Environmental Chemistry, Department of Chemistry, Carleton University, Ottawa, Ontario K1S 5B6, Canada

D. C. Grégoire
Geological Survey of Canada, Department of Energy, Mines and Resources, Ottawa, Ontario K1A OE8, Canada

M. Lamoureux and T. Ly
Centre for Analytical and Environmental Chemistry, Department of Chemistry, Carleton University, Ottawa, Ontario K1S 5B6, Canada

The interference by magnesium chloride with the atomization of manganese in electrothermal atomic absorption spectrometry (ETAAS) has been investigated using electrothermal vaporization inductively coupled plasma mass spectrometry (ETV-ICP-MS). The ETV-ICP-MS allows the direct observation of the loss of manganese during the charring step, and thereby allows differentiation between the manganese loss during charring and the loss due to formation of molecular species during atomization. The mechanism of interference by magnesium chloride is dependent on the charring temperature. At temperatures above 700 °C, the manganese is lost during charring; this loss occurs as the magnesium chloride matrix undergoes hydrolytic decomposition, and the manganese is carried away from the graphite furnace with the hydrogen chloride gas generated by the hydrolysis reaction. At charring temperatures lower than 700 °C the suppression in the manganese atomic absorption signal is due to a vapour-phase interference caused by formation of manganese chloride during atomization. The addition of ascorbic acid, as a chemical modifier, removes interferences in both the higher and the lower charring temperature regions. The results obtained by ETV-ICP-MS show that, for charring temperatures above 700 °C, ascorbic acid prevents the loss of manganese during charring. This effect is explained by retardation of hydrolysis of the magnesium chloride matrix by the chemical modifier, ascorbic acid.

Keywords: *Atomic absorption spectrometry; electrothermal atomization; inductively coupled plasma mass spectrometry; manganese; chloride interference*

Chloride matrices interfere with the determination of many elements by electrothermal atomic absorption spectrometry (ETAAS). Although the addition of nitric acid to aqueous solutions of samples to give a pH of 1.5 completely removes the interference of chloride matrix in the determination of some elements (zinc, manganese and iron),[1] for solid sampling it is necessary to know the cause of the chloride matrix interference in order that remedial action can be taken in direct analysis (without sample dissolution) of solid samples containing chloride matrices. However, of more fundamental importance is the fact that knowledge and understanding of reactions between various chloride species, analyte species and chemical modifiers in graphite furnaces are essential for the systematic development of graphite furnace technology.

Different theories have been proposed to explain the cause of chloride matrix interferences. These include: (*i*) loss of analyte during the charring step;[2,3] (*ii*) occlusion of the analyte in microcrystals of the chloride matrix which are expelled from the furnace during atomization;[4] (*iii*) expulsion of analyte from the furnace as a result of expansion of gaseous products released by the decomposition of matrix during atomization;[3,5] and (*iv*) interferences caused by formation of stable gaseous molecular chloride species which are not completely dissociated during atomization.[6–8] Using dual cavity platform atomization experiments, Welz *et al.*[3] have shown that the mechanisms of chloride matrix interference may depend not only on the temperature of the charring cycle (thermal pre-treatment step) but, more importantly, on the identity of the chloride matrix. These results showed, for example, that the interference caused by hydrated nickel chloride, $NiCl_2 \cdot 6H_2O$, which hydrolyses at elevated temperatures is different from that caused by sodium chloride which does not hydrolyse even on heating.

Although the mechanisms of some of these chloride interferences might not be understood, and can, in fact, vary with different analytes and interfering species, various methods have been developed to control them. These include use of inorganic chemical modifiers such as nitric acid,[1,2,9] the constant temperature furnace,[10] addition of hydrogen to the argon purge gas during charring and atomization,[11] addition of sulfuric acid,[9] phosphoric acid[12]

*Presented at the XXVII Colloquium Spectroscopicum Internationale (CSI) Pre-Symposium on Graphite Atomizer Techniques in Analytical Spectroscopy, Lofthus, Norway, June 6–8, 1991.

†To whom correspondence should be addressed.

and ammonium nitrate.[13] Two of the most successful approaches to the elimination of chloride interferences, particularly with high chloride concentrations, have been the use of the stabilized temperature platform furnace,[14] in conjunction with suitable chemical modifiers,[12,15] or for tube wall atomization the addition of organic modifiers.[16,17] Tominaga and Umezaki[16] showed that the addition of a 5% m/v solution of ascorbic acid to a solution containing manganese in 1% m/v sodium chloride gave 100% recovery of the analyte signal. Hydes[17] completely eliminated the effect of chloride interferences in the direct determination of manganese in sea-water samples, using addition of 1% m/v ascorbic acid, although some small residual peak height depression was observed for cobalt and copper with the added ascorbic acid.

The mechanism by which ascorbic acid removes chloride matrix interferences at high chloride concentrations where the ratio of chloride to analyte is in excess of 1×10^5:1 is not fully known. Regan and Warren[18] proposed that pyrolysis of ascorbic acid leaves a carbon residue on the graphite tube surface, which enhances the reduction of metal oxides during atomization. However, Hydes[17] discounts this theory as oxalic acid, which pyrolyses without leaving a residue, is equally effective at removing chloride interferences with copper analyte in sea-water samples.

Recently, Gilchrist *et al.*[19] have elucidated the effect of ascorbic acid on the appearance temperatures, peak height and integrated absorbance of lead and five other elements.[20] The effect on the lead absorbance profile was attributed to gas phase chemical modification caused by the release of hydrogen and carbon monoxide by pyrolysis of ascorbic acid during atomization. By coupling a gas chromatograph with a graphite furnace, these workers[19] showed that hydrogen and carbon monoxide, in excess of 1% v/v, were released by ascorbic acid into the furnace during atomization. When argon purge gas was mixed with equivalent amounts of these gases, the effect on appearance temperature and integrated absorbance for lead was the same as that obtained by the addition of ascorbic acid, confirming the gas phase chemical modification mechanism. Where atoms are formed by dissociation of gaseous oxide molecules, the oxygen levels are lowered by reaction with the released hydrogen and carbon monoxide, causing a shift in the peak appearance temperature to a lower temperature. However, in these experiments the samples contained only 1% v/v nitric or hydrochloric acid as a matrix, so that the amount of interferent released during atomization was very small, originating only from the decomposition of the analyte compound itself, or from the small amounts of the acid retained by the graphite tube after the sample was dried.[21,22]

The objectives of this work were: (*i*) to distinguish between the chloride interference caused by loss of analyte in the charring cycle, and that caused by a gas phase interference mechanism during the atomization cycle; and (*ii*) to determine if a gas phase chemical modification mechanism, similar to that proposed by Gilchrist *et al.*[20] can account for the removal of the chloride interference by ascorbic acid in samples that contain high concentrations of metal chloride interferents.

Electrothermal vaporization inductively coupled plasma mass spectrometry (ETV-ICP-MS) was used in this work as a diagnostic technique for the following reason. The experimental evidence presented later shows that when manganese in a magnesium chloride matrix is determined by ETAAS, manganese is partially lost in the charring cycle (at $\approx$700 °C). It is suspected that manganese is lost by being blown out of the furnace by the HCl(g) generated by hydrolysis of $MgCl_2 \cdot 6H_2O$ at temperatures $\geqslant$700 °C. However, the commercial (conventional) graphite furnace with its single heated medium (graphite tube) serving two separate functions, vaporization and atomization, used for this study cannot determine whether the lost manganese is an atomic or molecular species, or whether it is a condensed- or vapour-phase species. This is because the temperature ($\approx$700 °C) at which the manganese loss is observed in ETAAS is too low for the atomic absorption signal of manganese to be observed. Diagnosis of this loss of manganese in ETAAS would have been possible if, instead of the commercially available (conventional) graphite furnace that has been used for this work, one were to employ a laboratory-made, detachable graphite tube and cup furnace which employs two separate power supplies, one for heating the graphite cup (for vaporization) and the other for heating the graphite tube (for atomization). Such a furnace would permit spatial and temporal separation of two separate processes; vaporization and atomization.[23,24] However, such a graphite furnace was not available for this work. The ETV-ICP-MS, with its spatial and temporal separation of the vaporization process (at the ETV) and ionization process (at the ICP), coupled with mass spectrometric detection (which gives extremely high sensitivity), offered a valuable diagnostic technique that can be used to determine readily the manganese lost as free atoms or in chemically combined form in the charring cycle (during vaporization). Differentiation between free or combined manganese can be achieved only by studying ETAAS data together with ETV-ICP-MS data. Electrothermal AAS is capable of detecting only atomic species whereas ICP-MS can detect ions produced from both atomic and molecular species. Also, the multi-element capability of ICP-MS allows simultaneous determination of the analyte and the matrix ions of manganese, magnesium and chlorine, which is required for elucidating mechanisms of manganese loss during the charring cycle (vaporization).

To determine if a gas phase chemical modification mechanism was responsible for the effect of ascorbic acid addition, experiments, similar to those described by Gilchrist *et al.*,[20] were conducted in which the argon purge gas was mixed with hydrogen, in amounts similar to those produced by pyrolysis of the added ascorbic acid. In addition, the amounts of magnesium and chlorine remaining in the furnace after charring, but prior to the atomization step, were determined. These experiments quantified the amount of matrix removed during the charring cycle, and, for the magnesium chloride matrix, determined the extent of hydrolysis during the charring step. The residual amounts of magnesium were determined by flame AAS and chloride by ion chromatography.

Experimental

Apparatus

A Perkin-Elmer Model 5000 atomic absorption spectrometer equipped with a Zeeman background corrector and a heated graphite atomizer (HGA) Model 500 was used. Absorbance signals were recorded directly from the spectrometer. The absorbance *versus* time profiles were recorded with an IBM compatible computer using a software program TGP (Tech Graph Pad designed for scientists and engineers). The outputs were printed using a Hewlett-Packard Laser-Jet III printer. A Perkin-Elmer hollow cathode lamp for manganese and pyrolytic graphite coated graphite tubes (Perkin-Elmer Part No. B009-1504) were used. The temperature of the graphite tube was monitored with an Ircon Model 300c automatic optical pyrometer. Test solutions of 20 μl volumes were injected using a 20 μl Eppendorf pipette.

Gases

Argon gas of high purity (99.995% pure, Matheson Gas Products) was used both as the purge gas and the sheath gas.

Table 1 Experimental and operating conditions of the electrothermal atomizer used for atomization of manganese. The 1% v/v H_2 gas was added separately using another gas flow device

	Step					
Parameter	Dry*	Dry*	Char	Cool	Atomize	Clean
Temperature/°C	90	120	Variable	400	2500	2700
Hold time/s	40	20	40	3	5	3
Ramp time/s	10	5	10	2	1	1
Record/s	—	—	—	—	−2	—
Read/s	—	—	—	—	0	—
Baseline/s	—	—	—	—	−1	—
Internal gas flow/ml min^{-1}	300	300	300	300	50	300

*The two drying cycles were required to dry the sample completely in the graphite tube prior to the charring cycle.

The 5.0% v/v hydrogen gas in argon (supplied by Matheson Gas Products) was used to simulate the amount of hydrogen gas released from the pyrolysis of ascorbic acid. The hydrogen gas was diluted to the appropriate composition using a flow-meter regulator.

Standards and Reagents

Standards and reagents, in ultrapure water, were individually prepared as follows.

(*a*) *Stock solution of manganese* (1000 μg ml^{-1}). Prepared by dissolving 0.5026 g of manganese metal (99.94% pure, Fisher Scientific) in 10.00 ml of 1+1 HNO_3 (Ultrex, Baker) and diluting the solution to 500.00 ml with ultrapure water.

(*b*) *Dilute manganese solution* (5 μg ml^{-1}). Prepared by serial dilution of the 1000 μg ml^{-1} manganese stock solution with ultrapure water.

(*c*) *Magnesium chloride solution* (5% m/v). Prepared by dissolving 10.6700 g of $MgCl_2 \cdot 6H_2O$ (99.4% pure, Baker Analyzed Reagent) in 100.00 ml of ultrapure water.

Test solutions were prepared by serial dilution of the dilute manganese and the magnesium chloride solutions with ultrapure water in 25.00 ml calibrated flasks immediately prior to determination. The following solutions were prepared in ultrapure water: solution A, 0.02 μg ml^{-1} Mn+1% v/v HCl solution; solution B, 0.02 μg ml^{-1} Mn+1% v/v HCl+1% m/v $MgCl_2$ solution; solution C, 0.02 μg ml^{-1} Mn+1% v/v HCl+1% m/v $MgCl_2$+1% m/v ascorbic acid [the ascorbic acid was added by dissolving 0.2500 g of L-ascorbic acid (99.5% pure, Baker Analyzed Reagent) in ultrapure water]; solution D, 0.02 μg ml^{-1} Mn+1% v/v HCl+1% m/v $MgCl_2$+3% m/v ascorbic acid; solution E, 0.02 μg ml^{-1} Mn+1% v/v HNO_3; blanks for solutions A–D were prepared to contain only 1% v/v HCl (Ultrex, Baker) in ultrapure water; and the blank for solution E was prepared to contain only 1% v/v HNO_3 (Ultrex, Baker) in ultrapure water.

Ultrapure water was obtained direct from a Millipore-Q water purification system immediately prior to its use.

Experimental and Operating Conditions

The experimental and operating conditions used for the atomization of manganese are presented in Table 1. The manganese hollow cathode lamp was operated at a lamp current of 20 mA (the optimum lamp current recommended by the manufacturer). The most sensitive line, 279.5 nm, a spectral band pass of 0.2 nm (low slit) and an integration time of 7.0 s were used.

Determination of Residual Magnesium Chloride

Apparatus

A Perkin-Elmer Model 603 atomic absorption spectrometer equipped with an air–acetylene flame atomizer–burner and a deuterium arc background corrector, was used to determine the residual magnesium (as the chloride) that remained after the charring cycle. A magnesium hollow cathode lamp (Perkin-Elmer) was used. The most sensitive magnesium line, 285.2 nm, at a lamp current of 18 mA (which was below the optimum current recommended by the manufacturer), were used. The absorbance signals were recorded from the digital read-out of the spectrometer and were then corrected for blanks.

The chloride that remained after the charring cycle was determined using a Dionex Series 4000i ion chromatograph, equipped with an electrical-conductivity detector. The chromatograms were recorded with an SP4290 integrator. Aqueous solutions of the sample were loaded in a 50 μl sample loop using a 1 ml plastic syringe and were injected with an automatic injection device of the chromatograph.

Standards and reagents

A stock solution of 100 μg ml^{-1} of Cl^- was prepared by dissolving 0.1648 g of NaCl (Grade 1 Ultrapure, Johnson Matthey) in 1000.00 ml of ultrapure water.

Determination of the residual Cl^- in the extraction experiments required daily preparations of Cl^- standard solutions of various concentrations (0.1, 0.2, 0.5, 1.0, 2.0, 4.0, 6.0, 8.0, 10.0, 12.0 and 15.0 μg ml^{-1}) for the preparation of the calibration graphs.

A stock solution of 100 μg ml^{-1} of Mg was prepared by dissolving 0.1658 g of MgO (99.5% pure, Fisher Scientific) in 5.5 ml of concentrated HNO_3 (Ultrex, Baker) and diluting the solution to 1000.00 ml with ultrapure water.

Several standard solutions of various Mg concentrations (0.2, 0.5, 0.7, 1.0, 2.0 and 5.0 μg ml^{-1}) were prepared daily for the flame AAS determination of the residual Mg in the extraction experiments.

The experimental and operating conditions used for the determination of the residual magnesium chloride are presented in Table 2.

Table 2 Experimental and operating conditions for the determination of the residual magnesium chloride

	Step		
Parameter	Dry*	Dry*	Char
Temperature/°C	90	120	Variable
Ramp time/s	10	10	10
Hold time/s	30	20	40

*The two drying cycles were required to dry the sample completely in the graphite tube prior to the charring cyle.

Extraction procedure

Recovery and clean-up experiments were performed to ensure that the extraction procedure gave ≈100% recoveries of the residual magnesium (as the chloride) and to avoid possible contamination of the next sample by carry-over of measurable amounts of the analyte (magnesium or chloride) because of inadequate thermal treatment for clean-up of the graphite tube prior to its re-use.

Extractions of the magnesium chloride residue, with or without the added ascorbic acid, were performed in triplicate. The magnesium chloride matrix was charred at various temperatures using the operating procedures shown in Table 2. The residues were extracted by inserting the graphite tube (containing the residue) in 15 ml polystyrene tubes (Fisher Scientific), equipped with snap caps, in which solvents [in each polystyrene tube, 10.00 ml of dilute HNO_3 (pH≈3)] were pipetted. Each polystyrene tube, with its contents, was heated for 15 min at 70 °C and shaken for 5 min with a test-tube mixer (Vortex-Genie, Fisher Scientific). Each of these extracts was analysed for magnesium and chloride using flame AAS and ion chromatography, respectively.

ETV-ICP-MS Experiments

The inductively coupled plasma mass spectrometry (ICP-MS) instrument used for this work was a Perkin-Elmer/Sciex Elan Model 250, used in the positive ion detection mode. The extended quartz torch was used for all experiments. The ETV device was constructed in the laboratory and was of a design similar to that reported by Park and coworkers.[25,26] Fig. 1 shows a schematic diagram of the ETV device used. Several modifications were made to this device, including installation of an automatic optical pyrometer, Ircon Model 300c, to monitor the temperature of the vaporization surface of the electrothermal vaporizer, and use of specially designed graphite strips. The loss in the radiance transmission through the quartz cover was compensated for by adjusting the emissivity dial on the Ircon Model 300c. There was an 8% loss that was measured by monitoring the temperature at ≈800 °C with and without the quartz cover. The ETV device consisted of a resistively heated strip of graphite measuring 11×4×1 mm. The sample material vaporized from the graphite strip was transported to the plasma by a stream of argon, the flow of which was directed tangentially to the graphite support

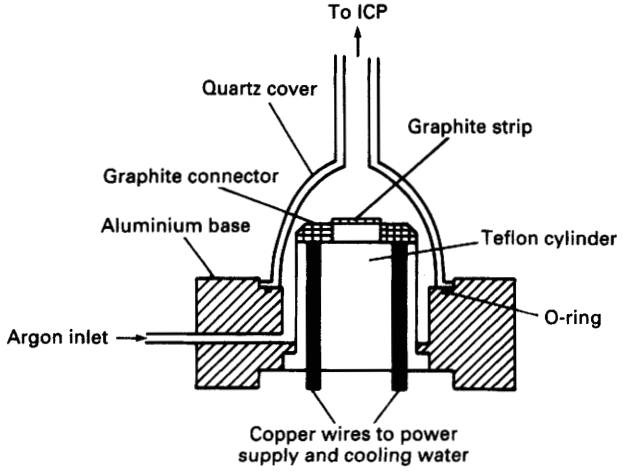

Fig. 1 Schematic diagram of the laboratory-made electrothermal vaporizer

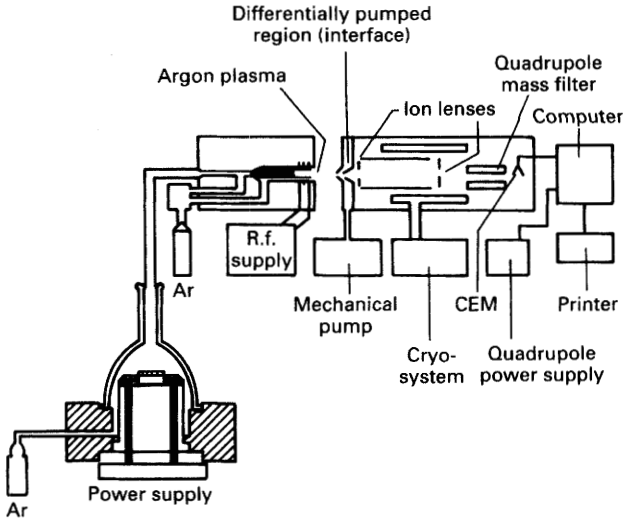

Fig. 2 Schematic diagram of the electrothermal vaporizer coupled to the inductively coupled plasma mass spectrometer

electrodes on which the graphite strip was mounted. A quartz cover resembling an inverted thistle tube was used to form an envelope above the vaporization surface. The tangential flow of argon gas and the shape of the quartz cover served to minimize condensation of the sample material (analyte and matrix components) on the quartz surface, and thus to maximize sample transport to the plasma. Fig. 2 shows a schematic diagram of the ETV device coupled to the ICP-MS instrument. The interface between the ETV unit and the ICP-MS instrument consisted of Tygon tubing, 1.0 m long, 6.0 mm i.d. connected directly to the plasma torch.

Pyrolytic graphite coated crystalline graphite (Ultra Carbon) was used to fabricate the graphite strips. A small oval-shaped depression was machined onto the surface of each strip at its centre. The depression served to hold the liquid sample and to prevent spreading of the sample during the drying step.

All instrumental parameter settings for the ETV-ICP-MS are given in Table 3.

Solutions of Mn, Mn plus $MgCl_2$ and Mn plus $MgCl_2$ plus

Table 3 Experimental and operating conditions for ETV-ICP-MS

Electrothermal vaporizer conditions and heating cycle—	Step		
Parameter	Dry	Char	Vaporize
Temperature/°C	110	Variable	2500
Ramp time/s	10	10	2
Hold time/s	60	40	10
Carrier gas flow rate	1.0 l min^{-1}		
Sample volume	10 μl		
Mass spectrometer interface—			
Sampler	Nickel, 1.14 mm orifice		
Skimmer	Nickel, 1.14 mm orifice		
Plasma conditions—			
R.f. power	0.9 kW		
Reflected power	5 W		
Auxiliary flow rate	2.0 l min^{-1}		
Nebulizer flow rate	0.7 l min^{-1}		
Plasma gas flow rate	12.5 l min^{-1}		
Sampling depth*	25 mm		

*Distance in millimetres from the tip of the mass spectrometer sampling cone to the downstream turn of the load coil.

ascorbic acid, were identical with the solutions for the ETAAS experiments except that in this instance they were prepared in 0.04% v/v HCl for the following reasons. The samples prepared in 1% v/v HCl occasionally spread towards the graphite electrode upon drying, which affected the reproducibility of the results and could be avoided by preparing all solutions in 0.04% v/v HCl. The ETV-ICP-MS signal for Cl was excessively large for 1% v/v HCl solutions, but much smaller for 0.04% v/v HCl solutions and the ETV-ICP-MS signal for Mn and Mg were identical for both the 1% v/v and the 0.04% v/v HCl solutions. Test solutions of 10 μl volumes were injected onto the graphite strip using a 10 μl Eppendorf pipette.

Results and Discussion

The ETAAS was performed by atomization from the graphite tube wall of the graphite furnace. This was in order to maximize the effects of the magnesium chloride matrix interference, providing more scope for study of interference mechanisms and their removal than would have been the case if these effects were minimized by use of atomization from a graphite platform. Moreover, the use of a graphite platform for atomization would have made recovery studies of the residual amounts of magnesium chloride in the furnace after the charring step more difficult because the matrix would then have been distributed between both the platform and the cooler parts of the tube wall after the charring cycle, making the washing out of the residue more difficult.

Fig. 3 shows the charring (A) and the atomization (B) curve for 400 pg of manganese plus 200 μg of magnesium chloride in 1% v/v HCl solution. Fig. 4 shows charring curves for manganese alone (A), manganese plus $MgCl_2$ (B), manganese plus magnesium chloride plus various amounts of ascorbic acid (C and D). The charring curve for manganese in 1% HNO_3 (E) is shown as a reference point. It illustrates the manganese AA signal without the chloride interferences. Typical absorbance profiles for these solutions at a charring temperature of 900 °C are presented in Fig. 5. In Figs. 3 and 4, an unusual feature of the charring curve with the magnesium chloride matrix (A and B, respectively) is the pronounced maximum at a charring temperature of around 700 °C. Fig. 3 also shows that although manganese in the magnesium chloride matrix is lost at charring temperatures higher or lower than 700 °C, the manganese atomic absorption signal is not observed until the furnace has attained a temperature of 1800 °C (the appearance temperature for manganese in the magnesium chloride). As no manganese atomic absorption signal is observed below 1800 °C, the manganese must have been lost as a molecular species. The thermal stability of this manganese molecular species is reflected in the 1100 °C difference between the maximum in the charring curve (700 °C) and the onset of the atomization curve (1800 °C), and establishes the temperature range in which the manganese species is lost from the furnace. Fig. 4, curve B, shows that the manganese absorbance values increase with increasing charring temperature, as might be expected, up to 700 °C, but then drop dramatically as the charring temperature is increased beyond 700 °C, even though this temperature is well below the normal appearance temperature (1480 K)[27] of manganese alone. Charring curves showing similar maxima, in magnesium chloride matrices, have been reported for copper[9] and lead.[28] Fig. 4 also shows that the effect of the ascorbic acid chemical modifier is different both above and below the charring temperature of 700 °C. At concentrations of 1% m/v (*i.e.*, 200 μg ascorbic acid addition), ascorbic acid is effective in recovering 100% of the manganese absorbance at charring temperatures of 700 °C or above; below this temperature the magnesium

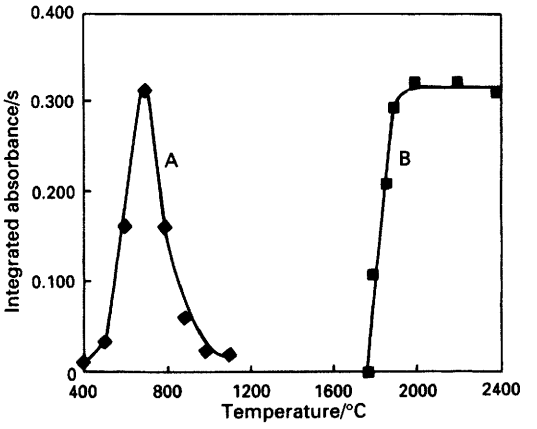

Fig. 3 A, Charring curve and B, atomization curve for 400 pg of Mn+200 μg of $MgCl_2$ in 1% v/v HCl. The optimum atomization temperature for the charring curve was 2400 °C and the optimum charring temperature for the atomization curve was 700 °C

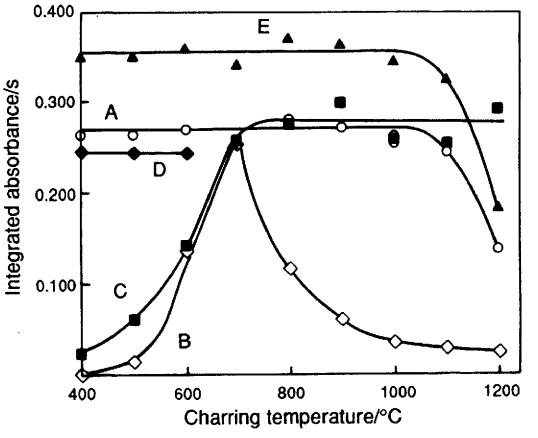

Fig. 4 Charring curves in ETAAS. A, 400 pg of Mn in 1% v/v HCl; B, A+200 μg of $MgCl_2$; C, B+200 μg of ascorbic acid; and D, B+600 μg of ascorbic acid; and E, 400 pg of Mn in 1% v/v HNO_3

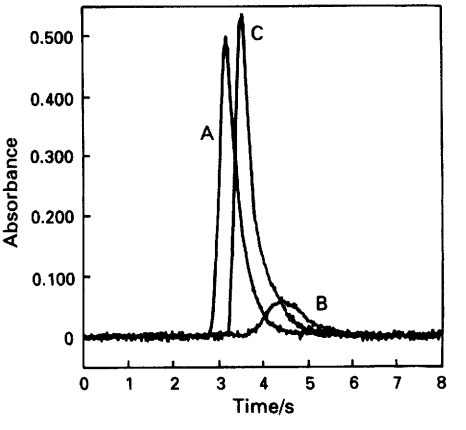

Fig. 5 Typical absorbance profiles in ETAAS at a charring temperature of 900 °C. A, 400 pg of Mn in 1% v/v HCl; B, A+200 μg of $MgCl_2$; C, B+200 μg of ascorbic acid

chloride interference is only partly removed. These results suggest that both the mechanism of the interference and its removal by ascorbic acid above 700 °C is different from that below 700 °C.

In order to establish whether the effect of the ascorbic acid chemical modifier, in either of these charring temperature regions, could be attributed to a gas phase chemical

modification mechanism, similar to that described by Gilchrist and co-workers,[19,20] the argon purge gas was mixed with 1% v/v hydrogen during the charring and atomization cycles. This hydrogen concentration is equivalent to that found to be released by pyrolysis of 100 μg of ascorbic acid in a graphite furnace, using similar charring temperatures and purge gas flow conditions.[19] The results of these gas phase modification experiments are given in Fig. 6. At charring temperatures below 700 °C, the added hydrogen removes the magnesium chloride interference only partially. This result is similar to that observed in Fig. 4 when the ascorbic acid chemical modifier has been added and suggests that the partial removal of the magnesium chloride interference at low charring temperatures is due to a gas phase chemical modification, in which some of the magnesium chloride remaining after the charring is removed during atomization *via* a gas-phase reaction of the type:

$$MgCl_2(g)+H_2(g)\rightarrow Mg(g)+2HCl(g)$$

Increasing the mass of ascorbic acid to 600 μg in the sample containing the manganese and the magnesium chloride matrix (Fig. 4, curve D) removes almost all the matrix interference. Increasing the mass of ascorbic acid is equivalent to increasing the concentration of hydrogen in the argon purge gas, which then allows more chloride to be removed by the hydrogen gas *via* a gas phase chemical modification mechanism at charring temperatures below 700 °C.

However, for charring temperatures above 700 °C, the results of the hydrogen addition experiments (Fig. 6) in no way parallel the results of the ascorbic acid addition (Fig. 4). Whereas the ascorbic acid chemical modifer causes complete removal of the magnesium chloride interference in this higher charring temperature range, additions of hydrogen has, in fact, a slight depressive effect on the manganese integrated absorbance signal. This would indicate that, in this temperature range, the mechanism by which ascorbic acid eliminates the magnesium chloride interference is not a gas-phase reaction, but one based on processes occurring in the condensed phase at the graphite surface during charring. Welz *et al.*[3] have differentiated chloride interferences arising from gas-phase reactions and from condensed-phase reactions at the graphite surface using atomization from a dual-cavity graphite platform. They have studied the effect of $NiCl_2{\cdot}6H_2O$ interferences with lead atomization, at concentrations similar to those used in the present work, and have concluded that the interferences are caused by loss of analyte during charring. They have proposed that these losses result from the hydrolysis reaction of the hydrated nickel chloride matrix known to occur at temperatures around 600 °C:[29] *i.e.*,

$$NiCl_2{\cdot}6H_2O(s)\rightarrow NiO(s)+2HCl(g)+5H_2O(g)$$

Welz *et al.* suggested that the above reaction results in covolatilization of the analyte, and its expulsion from the furnace together with the hydrogen chloride gas generated by the hydrolysis reaction.

Hydrated magnesium chloride is also known to hydrolyse up to 600 °C.[30,31] However, the mixed condensed phase ($MgCl_2$, MgOHCl, MgO) which is present at 600 °C[30] could hydrolyse at higher temperature releasing HCl gas. A mechanism similar to the one proposed by Welz *et al.*[29] that would involve hydrolysis of the magnesium chloride matrix and the loss of manganese carried away with the HCl(g) from the charring cycle hydrolysis reaction would explain the sharp decrease in the absorbance signal of manganese observed in the charring curve of Fig. 4 at temperatures above 700 °C. Moreover, it would also explain why hydrogen, added to the argon purge gas, is ineffective in restoring the manganese signal at charring temperatures above 700 °C: if the analyte has been already lost from the furnace during charring, then no gas-phase reaction during atomization could be expected to recover the manganese signal. The manganese atomic absorption signal is not observed when the magnesium chloride matrix is present until a temperature of at least 1800 °C (Fig. 3) is attained. It is necessary to determine experimentally how this manganese is lost. As explained earlier, ETV-ICP-MS offers a promising diagnostic technique for investigation of the loss of manganese in the charring cycle.

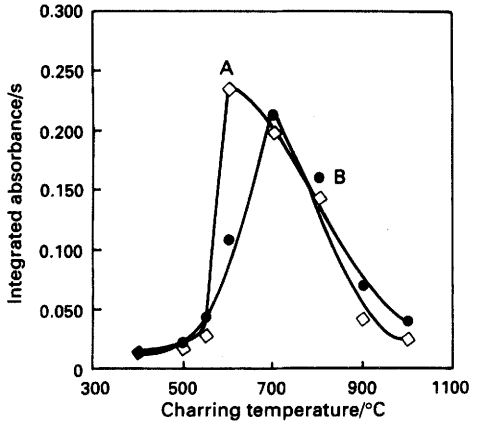

Fig. 6 Charring curves in ETAAS. A, 400 pg of Mn in 1% v/v HCl+200 μg of $MgCl_2$+argon containing 1% v/v H_2 gas; B, 400 pg of Mn in 1% v/v HCl+200 μg of $MgCl_2$+argon gas

ETV-ICP-MS Experiments

In these experiments, the manganese in the magnesium chloride matrix, with and without the ascorbic acid chemical modifier, was vaporized from a graphite strip electrothermal vaporizer, and the vapour generated, both during the charring and the atomization step, transported to the ICP-MS instrument. Details of the experimental procedure are given under Experimental. Any molecular chloride analyte species, produced either during the charring or the atomization step, were dissociated in the argon plasma to yield manganese atoms which were then ionized in the plasma and detected as manganese atomic ions by the mass spectrometer.[32] This technique allows detection of analyte during both the charring and the atomization step as a function of the temperature of the vaporizing graphite strip (ETV). For each sample tested, the ETV-ICP-MS signals for $^{55}Mn^+$, $^{37}Cl^+$ and $^{25}Mg^+$ were recorded simultaneously; no memory effect was detected for any of the three ions.

Figs. 7–9 show $^{55}Mn^+$ ETV-ICP-MS signals for manganese in various matrices and at different charring temperatures. The temperature of the graphite strip (ETV) surface during the charring and the vaporization step is also shown. The temperature of the graphite strip (ETV) is also shown to increase after the end of the heating ramp during the charring cycle. Therefore, the temperature of the graphite strip (ETV) will be reported as a temperature range which covers the last 25 s of the charring cycle. The charring and the vaporization steps for each figure are from 0 to 40 s and 40 to 50 s, respectively. Fig. 7 shows the $^{55}Mn^+$ signal for 200 pg of manganese in 0.04% v/v HCl at charring temperatures of 500–600 °C [Fig. 7(*a*)] and 700–900 °C [Fig. 7(*b*)]. The manganese peak, centred at about 42 s for both charring temperatures, 500–600 and 700–900 °C, appears in the vaporization step and has approximately the same peak area (integrated ion intensity) for both charring temperatures. The peak area sensitivity can only be interpreted qualitatively since the effects of the various matrices (especially magnesium) on the mass transport efficiency and

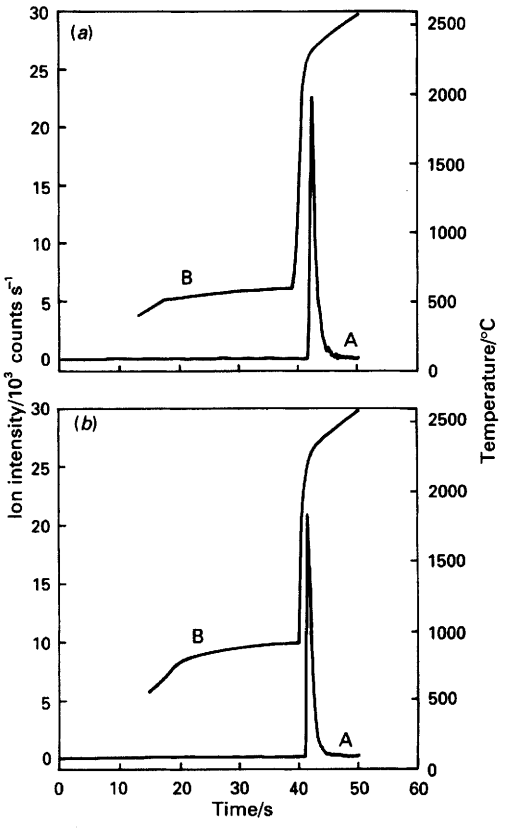

Fig. 7 Temporal behaviour of $^{55}Mn^+$ in ETV-ICP-MS in various matrices as a function of the temperature of the graphite strip: (*a*) 500–600 °C; and (*b*) 700–900 °C. A, 200 pg of Mn in 0.04% v/v HCl; and B, temperature profile of the graphite strip

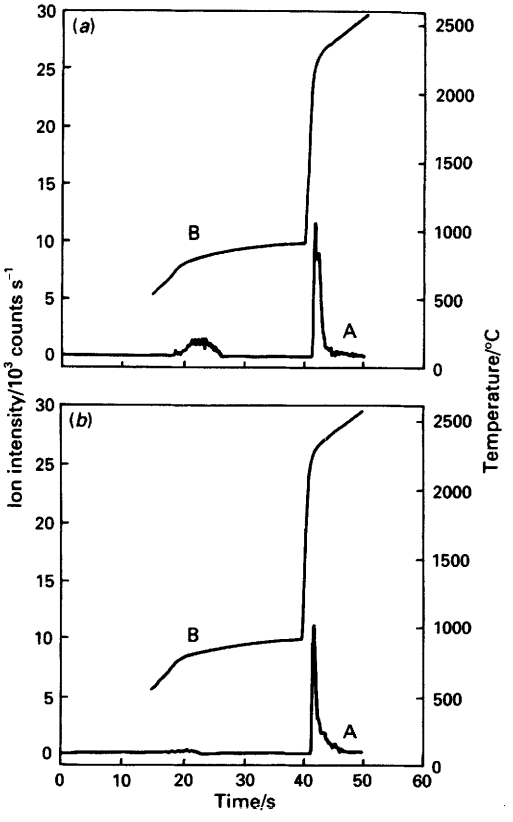

Fig. 8 Temporal behaviour of the $^{55}Mn^+$ in ETV-ICP-MS in various matrices at a temperature of 700–900 °C for the graphite strip. A, 200 pg of Mn in 0.04% v/v HCl; and B, temperature profile of the graphite strip. (*a*) 100 μg of $MgCl_2$; and (*b*) 100 μg of $MgCl_2$ + 100 μg of ascorbic acid

plasma properties, which affect the ion counts are not yet fully understood. During the charring step, no manganese peak is observed for any of the above charring temperatures, indicating that no manganese is evolved before the vaporization step from the ETV device.

At a charring temperature of 700–900 °C, the addition of 100 μg of magnesium chloride [Fig. 8(*a*)] and 100 μg of magnesium chloride plus 100 μg of ascorbic acid [Fig. 8(*b*)] to 200 pg of manganese in 0.04% v/v HCl shows siginficantly different ETV-ICP-MS profiles for manganese. The sample without the ascorbic acid shows a manganese peak centred around 23 s during the charring cycle [Fig. 8(*a*)], indicating that the manganese is evolved (or lost) from the sample during the charring cycle. The temperature that corresponds to the centre of the manganese peak at 23 s is 800 °C. The manganese peak observed at 23 s in Fig. 8(*a*) provides convincing evidence that the chloride interference in ETAAS is caused by the manganese loss during the charring cycle at 800 °C. Moreover, the above mechanism explains why, in the earlier ETAAS experiments, hydrogen gas was ineffective in restoring the manganese signal at charring temperatures above 700 °C. A gas phase reaction mechanism in ETAAS could only be expected to reduce interferences caused by the formation of molecular chloride species in the gas phase, but would do nothing to prevent the manganese loss by expulsion during the charring cycle. The manganese peak centred at 23 s in Fig. 8(*a*) (at a temperature of 800 °C) accounts for approximately 39% of the total manganese signal, *i.e.*, 39% loss of manganese in the charring cycle. In ETAAS, at a charring temperature of 800 °C, the AA signal for manganese in the presence of the magnesium chloride matrix (Fig. 4, curve B) was reduced to 58% of that observed without magnesium chloride matrix, *i.e.*, 42% manganese loss in the charring cycle. The addition of ascorbic acid reduces the manganese loss during the charring cycle [Fig. 8(*b*)] and only a trace amount of manganese at 23 s can be observed. This result is in agreement with those shown in Fig. 4 where for charring temperatures above 700 °C, the addition of ascorbic acid removes the matrix interference completely. Thus, in ETAAS, in the above charring temperature range, the ascorbic acid removes the matrix interference by preventing the manganese loss during the charring cycle; a mechanism to account for this will be proposed in the next section.

The ETV-ICP-MS experiments were conducted at charring temperatures below 700 °C in order to elucidate the interference mechanism in this low temperature charring region. The results for a charring temperature of 500–600 °C are given in Fig. 9. At this temperature, no loss of the manganese in the magnesium chloride matrix was observed during charring periods of <40 s (Fig. 9), which means that at this lower charring temperature the matrix interference was not caused by manganese evolved from the graphite strip (ETV) during the charring. Moreover, a comparison of Figs. 7(*a*) and 9 shows that the amount of manganese released during the vaporization is similar both in the presence and in the absence of the magnesium chloride matrix. This result contrasts with the absorbance profiles obtained using graphite furnace atomization (Fig. 10), in which considerable suppression of the absorbance signal occurred in the presence of the magnesium chloride matrix (Fig. 10, curve B). The conclusion reached from Figs. 9 and 10 is inescapable since the ETV-ICP-MS results confirm that no loss of manganese occurred during the charring step and the suppression of the absorbance signal observed in graphite furnace atomization (Fig. 10) must be due to the formation of molecular manganese species (probably man-

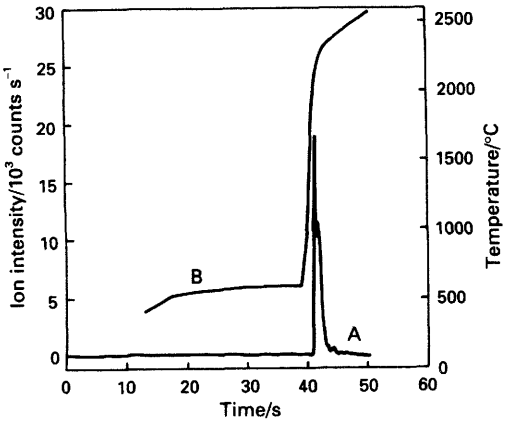

Fig. 9 Temporal behaviour of the $^{55}Mn^+$ in ETV-ICP-MS at a charring temperature 500–600 °C of the graphite strip. A, 200 pg of Mn^+ +100 μg of $MgCl_2$ in 0.04% v/v HCl; and B, temperature profile of the graphite strip

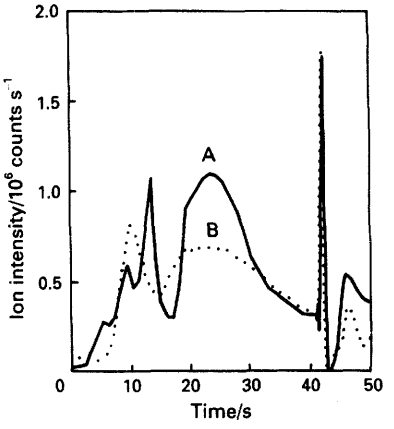

Fig. 11 Temporal behaviour of $^{37}Cl^+$ in ETV-ICP-MS in various matrices at a temperature of 500–600 °C of the graphite strip. A, 200 pg of Mn in 0.04% v/v HCl+100 μg of $MgCl_2$; and B, A+100 μg of ascorbic acid

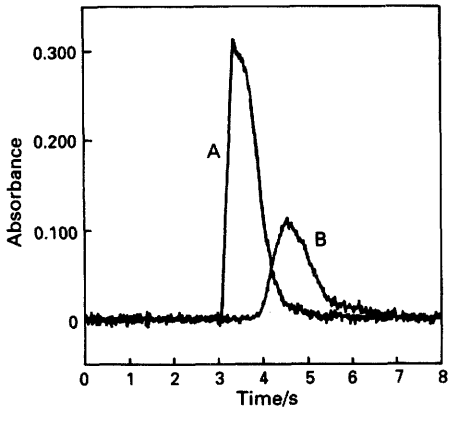

Fig. 10 Absorbance profiles of Mn in ETAAS at a charring temperature of 600 °C. A, 400 pg in 1% v/v HCl; and B, A+200 μg of $MgCl_2$

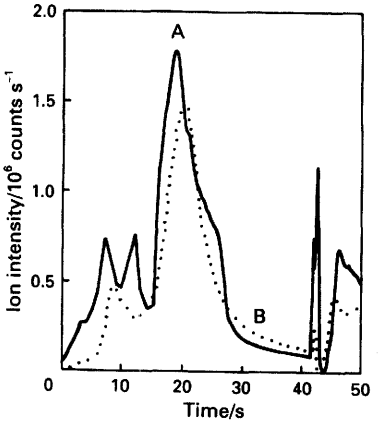

Fig. 12 Temporal behaviour of $^{37}Cl^+$ in ETV-ICP-MS in various matrices at a temperature of 700–900 °C of the graphite strip. A, 200 pg of Mn in 0.04% v/v HCl+100 μg of $MgCl_2$; and B, A+100 μg of ascorbic acid

ganese chloride) which remains undissociated at the low temperature, producing no detectable manganese atomic absorption. These same molecular species formed during vaporization from the graphite strip in the ETV experiments, but they were subsequently dissociated in the high-temperature plasma, and detected as atomic manganese ions by the mass spectrometer, giving rise to the same signal obtained in the absence of the magnesium chloride matrix.

Figs. 11 and 12 show the $^{37}Cl^+$ ETV-ICP-MS signals that correspond to Figs. 9 and 8, respectively. The figures were drawn using data corrected for blanks, and show only the net $^{37}Cl^+$ signal produced by the magnesium chloride matrix. Figs. 13 and 14 show the corresponding $^{25}Mg^+$ ETV-ICP-MS signals for Figs. 9 and 8. At charring temperatures between 500 and 600 °C, Fig. 13, no magnesium is observed during the charring period (20–40 s), which means that the chlorine observed in the corresponding region of Fig. 11 must be due solely to HCl produced by the onset of the matrix hydrolysis reaction. Fig. 11 also shows that more chloride is released during charring (20–40 s) when no ascorbic acid is present (curve A). This suggests that ascorbic acid inhibits the magnesium chloride matrix hydrolysis reaction. The Cl signal in the range of 4–14 s and the corresponding magnesium signal of Fig. 13 is probably due to magnesium chloride crystals ejected during the temperature ramping at the beginning of the charring cycle (this has been observed several times). The most interesting feature of Fig. 11 is the sharp Cl peak, at approximately 42 s, during the vaporization cycle. This peak has an appearance time coincident with the manganese peak of Fig. 9, and appears at a temperature of around 1500 °C, somewhere during the temperature ramp after charring. Therefore, the peak could be attributed to residual magnesium chloride vaporized at its boiling-point of 1480 °C. This peak has an identical shape and ion intensity both in the presence and absence of the ascorbic acid chemical modifier. The identical peak areas would suggest that manganese in both solutions was subjected to the same amount of chloride interference during the vaporization of Mn, and that the interference by chloride with manganese is of the same magnitude in the magnesium chloride matrix with and without the ascorbic acid chemical modifier. This is in agreement with the ETAAS results where the manganese integrated absorbance values are similar for magnesium chloride with and without the ascorbic acid for charring temperatures <700 °C (Fig. 4, curves B and C), indicating that both solutions suffer the same degree of chloride interference. The broader Cl peaks observed in the range of 44–50 s occur at a higher temperature (≈2400 °C) and could be due to the release of Cl trapped in the MgO lattice.

The Cl signal from Fig. 12 exhibits a similar trend as in Fig. 11 in the range of 4–14 s. This is probably due to the same effect as described earlier. The Cl peak intensity at a charring temperature of 700–900 °C in the range of 16–30 s for the magnesium chloride matrix without the ascorbic acid (Fig. 12, curve A) is about 1.7 times greater than at a charring temperature of 500–600 °C (Fig. 11, curve A), and

for the magnesium chloride matrix with ascorbic acid (Fig. 12, curve B) it is 2.3 times greater than at a charring temperature of 500–600 °C (Fig. 11, curve B). However, the Cl peak area in the absence of ascorbic acid is still larger, suggesting that the extent of hydrolysis of magnesium chloride is greater when no ascorbic acid is present. The Cl peaks at 42 s for the magnesium chloride matrix with and without the ascorbic acid have different intensities and both Cl peaks are smaller compared with the Cl peak in Fig. 11 at 42 s. The Cl peak intensity is decreased about 9-fold in the magnesium chloride matrix with ascorbic acid whereas the Cl peak intensity from the matrix without ascorbic acid decreases only about 1.6-fold. This result indicates that ascorbic acid not only prevents manganese loss during the charring cycle, but also reduces the amount of chloride present during the vaporization of manganese at 42 s.

Figs. 13 and 14 show the $^{25}Mg^+$ ETV-ICP-MS signal corresponding to Figs. 9 and 8, respectively. Because of the very high sensitivity of ICP-MS for magnesium, which produces a signal near the upper limit of the linear dynamic range of the detector, the interpretation of the Figs. 13 and 14 can only be made qualitatively. In both Figs. 13 and 14, an off-scale magnesium peak in the range of 40–50 s was observed and was due to residual manganese chloride remaining after the charring cycle, which was vaporized early in the vaporization cycle, and to magnesium oxide (produced by the hydrolysis of magnesium chloride), which vaporized at a much higher temperature. The magnesium peaks observed in both Figs. 13 and 14 in the range of 0–14 s were due to the sample material ejected from the graphite strip during the temperature ramping in the charring cycle. The important distinction between Figs. 13 and 14 is the magnesium peak centred at 24 s which appears in Fig. 14. The magnesium peak at 24 s appeared at the same time as the manganese peak in Fig. 8(*a*). The hydrolytic decomposition of magnesium chloride matrix without ascorbic acid was observed experimentally to be a violent reaction (as in an explosion) which releases HCl(g). This release of HCl(g) could have expelled the manganese and the matrix components from the ETV device and therefore the magnesium peak at 24 s was due to magnesium molecular species carried away with the HCl(g) generated by the hydrolytic decomposition of the matrix. The apparently high intensity of this magnesium peak should be kept in perspective, considering the large amount of magnesium chloride in the sample. If only 2% of the 100 μg sample of magnesium chloride is carried over during the hydrolysis reaction, this would correspond to 0.5 μg of magnesium, sufficient to cause an off-scale peak given the high sensitivity of magnesium. However, this small amount of covolatilized magnesium chloride would account for the shoulder at 24 s on the Cl peak (Fig. 12, curve A). This shoulder, which coincides with the centre of the magnesium peak, could result from the small amount of magnesium chloride carried over, whereas the major part of this Cl peak, which precedes the release of magnesium, probably comes from HCl(g) produced by the hydrolytic decomposition of the magnesium chloride matrix. Except for the magnesium peak observed in the range of 18–30 s, no other magnesium peak originating from magnesium chloride vaporized during the charring cycle could contribute to the Cl signal in Figs. 11 and 12; therefore, the Cl signals at times less than 18 s and greater than 30 s must be due to HCl(g) released by the hydrolytic decomposition of the matrix with and without the ascorbic acid, although in a smaller amount for the ascorbic acid containing solutions.

The $^{37}Cl^+$ and the $^{25}Mg^+$ ETV-ICP-MS signals in Figs. 11–14 provide experimental evidence for the hydrolysis of magnesium chloride. Fig. 13, curve A, shows that at 500–600 °C there is no magnesium signal, and hence, magnesium chloride cannot be the source of the observed

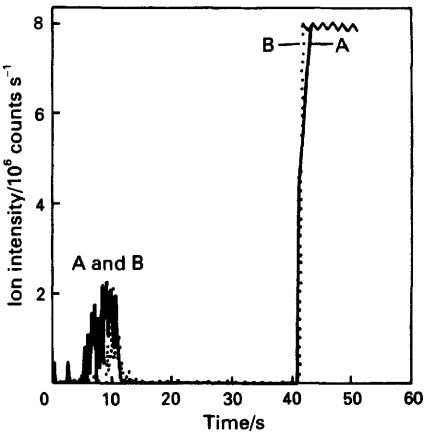

Fig. 13 Temporal behaviour of $^{25}Mg^+$ in ETV-ICP-MS in various matrices at a temperature of 500–600 °C of the graphite strip. A, 200 pg of Mn in 0.04% v/v HCl + 100 μg of $MgCl_2$; and B, A + 100 μg of ascorbic acid

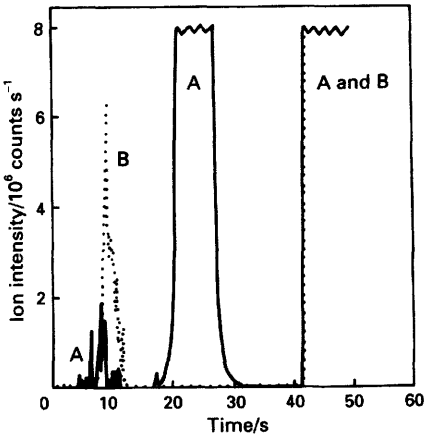

Fig. 14 Temporal behaviour of $^{25}Mg^+$ in ETV-ICP-MS in various matrices at a temperature of 700–900 °C of the graphite strip. A, 200 pg of Mn in 0.04% v/v HCl + 100 μg of $MgCl_2$; and B, A + 100 μg of ascorbic acid

Cl signal in Fig. 11, curve A. In Fig. 11, curve A, the only other possible source of the Cl signal is HCl(g), which, at 500–600 °C probably arises from the incipient hydrolysis of magnesium chloride, producing HCl(g) over a wide time interval (20–40 s); the width of the time interval is indicative of the slow hydrolysis of $MgCl_2$(s) at this low temperature. At 700–900 °C, Fig. 12, curve A, shows a greater Cl peak intensity in the 18–28 s range compared with the Cl signal in Fig. 11, curve A, (500–600 °C). In Fig. 12, curve A, neglecting the Cl shoulder (24–28 s) that originates from the $MgCl_2$(s) carried away by HCl(g) (Fig. 14, curve A, 20–30 s, shows the corresponding $^{25}Mg^+$ peak), most of the Cl signal probably arises from vigorous hydrolysis of magnesium chloride at 700–900 °C; also, the fact that the Cl signal is higher in intensity and covers a much smaller time interval (16–24 s) than the Cl signal (20–40 s) in Fig. 11, curve A, suggests that the hydrolysis of $MgCl_2$(s) is much more vigorous at 700–900 °C than at 500–600 °C. The ETV-ICP-MS thus presents valuable evidence for hydrolysis of $MgCl_2$, resulting in formation of HCl(g).

Use of ETV-ICP-MS as a diagnostic technique permits the two different mechanisms for chloride interference outlined by Welz *et al.*[3] to be distinguished experimentally, *i.e.*, chemical interference caused by the formation of molecular analyte species during atomization and chemical

interference caused by analyte loss during charring in ETAAS. In addition, it explains the unusual shape of the charring curves of Fig. 4. In this system, and presumably for many other hydrated salt matrices, the interference mechanism is dependent on the charring temperature chosen. If the charring temperature is greater than the hydrolytic decomposition temperature of the metal chloride matrix, then extensive analyte loss caused by expulsion with the gases produced by the hydrolytic decomposition of the metal chloride matrix will occur. At charring temperatures below 700 °C, the magnesium chloride matrix hydrolysis reaction does not occur, or occurs slowly, and hence, little analyte is lost. However, very little of the magnesium chloride matrix will be removed by charring at these lower temperatures, resulting in the release of relatively large amounts of residual chloride from the matrix during the atomization step and, as a consequence, chemical interference by formation of molecular manganese chloride species during atomization. The optimum charring temperature of around 700 °C for the manganese in the magnesium chloride matrix (Fig. 4) is one where the maximum amount of the matrix is removed from the furnace by vaporization prior to the onset of the matrix hydrolysis reaction.

Mechanism of Removal of the Interference by Ascorbic Acid

Results of the ETV-ICP-MS experiments have shown that ascorbic acid chemical modifier inhibits the loss of manganese during charring at temperatures above 700 °C. If the manganese is lost by being carried away with the products of the hydrolytic decomposition reaction of the magnesium chloride matrix, it is likely that the ascorbic acid prevents such loss by inhibiting or retarding this hydrolysis reaction during the charring step. To test this hypothesis, the extent of hydrolysis of the magnesium chloride matrix after charring at various temperatures was determined, both in the presence and in the absence of ascorbic acid chemical modifier. To do this, the amounts of magnesium and chloride residue remaining in the tube immediately after the charring cycle (but prior to atomization) were determined. The graphite furnace heating cycle was interrupted after the charring cycle, the furnace allowed to cool, and the residual matrix dissolved in 0.001 mol dm^{-3} nitric acid. This solution was then analysed for magnesium by flame AAS and for chloride by ion chromatography.

Fig. 15 shows how the residual amounts of magnesium and chloride, both in the presence and in the absence of ascorbic acid chemical modifier, change as a function of the charring temperature. These results are the mean of three replicates. The test solutions analysed were identical with those used to obtain the charring curves of Fig. 4, *i.e.*, 20 ml solutions containing 200 μg of magnesium chloride with or without 200 μg of ascorbic acid.

The effect of ascorbic acid on the hydrolysis reaction of the magnesium chloride matrix during charring can be interpreted as follows. If the hydrolysis of the magnesium chloride matrix goes to completion *via* the reaction

$$MgCl_2 \cdot 6H_2O(s) \rightarrow MgO(s) + 2HCl(g) + 5H_2O(g)$$

then all of the chloride would be removed from the furnace as HCl(g) during charring, and almost all of the magnesium would remain in the furnace, since the vapour pressure of solid magnesium oxide would be expected to be extremely low at these relatively low charring temperatures. Hence, a large degree of hydrolysis would be indicated by low residual chloride, high residual magnesium and a high ratio of residual magnesium to chloride. If, on the other hand, the hydrolysis does not go to completion, or is retarded by the addition of ascorbic acid, then less hydrogen chloride would be evolved during charring, and the amount of chloride remaining in the furnace after the charring would

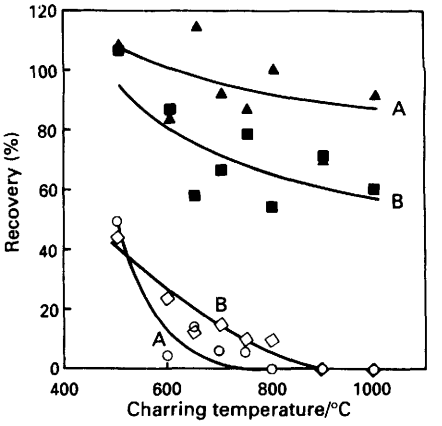

Fig. 15 Percentage of residual magnesium and chloride as a function of the charring temperature. A, 200 μg of $MgCl_2$; and B, 200 μg of $MgCl_2$ + 200 μg of ascorbic acid; Mg (closed symbols) and Cl (open symbols)

be higher. Moreover, since the melting- and boiling-points of $MgCl_2$(s) are much lower than those of MgO(s), it would be expected that some of this unhydrolysed $MgCl_2$(s) would be removed during the charring, resulting in a lower residual magnesium level when ascorbic acid is present. The results of Fig. 15 confirm this: when ascorbic acid chemical modifier is present at a charring temperature above the onset of the hydrolysis reaction, *i.e.*, around 600 °C, the amount of residual chloride is higher, and the amount of residual magnesium lower. However, a better indicator of the extent of magnesium chloride hydrolysis during charring is the molar ratio of residual magnesium to chloride. This ratio is 0.5 in unhydrolysed magnesium chloride, and will increase with increasing extent of hydrolysis, attaining very high values as the hydrolysis reaction approaches completion. The retardation effect of ascorbic acid on the hydrolysis reaction is clearly illustrated by Fig. 16. At charring temperatures above 700 °C, when no ascorbic acid is present, the molar ratio of magnesium to chloride increases sharply, rising to around 250 at 1000 °C. The addition of ascorbic acid by retarding the hydrolysis reaction reduces this ratio significantly, *e.g.*, at 800 °C, the molar ratio is reduced from 100 to 3.

Kántor and Bezúr[31] have also investigated the effect of ascorbic acid on the hydrolytic decomposition of magnesium chloride, in the same temperature range, using a quartz furnace vaporizer coupled to a flame atomic absorption spectrometer. Samples were heated from 100 to 900 °C at a slow heating rate (0.8–20 K s^{-1}) and the magnesium atoms formed by matrix decomposition were monitered by flame AAS. Although these workers expected that the addition of ascorbic acid would result in a 'decrease in the adsorption hydrolysis of magnesium chloride', they reported that 'experience contradicted this expectation'. This conclusion was based solely on the determination of the amount of magnesium atoms formed during the heating, rather than on the determination of both magnesium and chloride, as has been done in the present experiments. They concluded that less hydrolysis had occurred in the absence of ascorbic acid, as more magnesium was observed under these conditions. However, the above conclusion would be erroneous, if, during the vigorous hydrolysis reaction, some of the magnesium chloride matrix was carried away and expelled from the furnace with the hydrogen chloride gas, in the same manner as has been proposed for the manganese analyte [Fig. 8(*a*)] and the magnesium chloride matrix (Fig. 4). Such expulsion of a small part of the magnesium has been observed repeatedly in the ETV-ICP-MS experi-

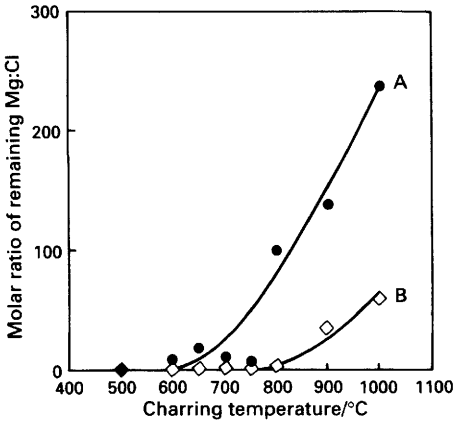

Fig. 16 Molar ratio of magnesium to chloride remaining after charring as a function of the charring temperature. A, 200 μg of $MgCl_2$; and B, 200 μg of $MgCl_2$+200 μg of ascorbic acid

ments when no ascorbic acid chemical modifier was present.

The precise mechanism responsible for the retardation of the hydrolysis of the magnesium chloride matrix by ascorbic acid is not known, and is beyond the scope of this paper. However, observations of the manganese in the magnesium chloride matrix system during charring in the graphite furnace, and especially on the ETV graphite strip are as follows. When no chemical modifier was present, the matrix dried to a white crystalline material and decomposed violently during charring, presumably as the hydrolysis reaction occurred. In the presence of ascorbic acid, the sample matrix formed a melt, in the drying step, which partially evaporated, in a much more controlled manner, during charring. Probably, ascorbic acid, a known bidentate ligand, forms a complex with the magnesium ions in this melt, facilitating the removal of water of hydration during the drying stage, and thereby retarding the hydrolysis reaction during the charring.

Conclusions

The interferences of magnesium chloride in the determination of manganese by ETAAS occur by two different mechanisms, depending on the charring temperature. If the charring temperature exceeds the temperature required for the hydrolytic decomposition of the magnesium chloride matrix then HCl(g) will be formed. Manganese will then be lost during charring by expulsion with rapidly expanding HCl(g). At charring temperatures below 700 °C, where minimal decomposition of the magnesium chloride matrix occurs, no manganese is lost during charring, but the manganese atomic absorption signal is suppressed because larger amounts of residual magnesium chloride are released into the vapour phase, resulting in the formation of undissociated gaseous manganese chloride in the atomization cycle. This interference is reduced as the charring temperature is increased up to 700 °C, presumably because more of the unhydrolysed magnesium chloride matrix is removed from the graphite furnace by vaporization at higher temperatures. The same mechanism should apply also to other hydrated chloride matrices which undergo rapid hydrolytic decomposition during charring producing HCl(g). This mechanism may be applicable also to the matrices containing chlorides which undergo rapid hydrolysis producing HCl(g). In such instances, the optimum charring temperature would be just below the matrix decomposition temperature at which the maximum amount of matrix is removed by vaporization prior to the onset of hydrolysis. In addition, in ETAAS, for atomization from the tube wall, ascorbic acid can be used as an effective chemical modifier. In ETAAS of manganese in the magnesium chloride matrix, at charring temperatures above 700 °C, ascorbic acid retards the hydrolysis reaction of the magnesium chloride matrix, and thus prevents loss of manganese during the charring cycle.

The authors are grateful to the Natural Sciences and Engineering Research Council of Canada and the Department of Energy, Mines and Resources for financial support for this research project.

References

1 Sturgeon, R. E., Berman, S. S., Desaulniers, A., and Russell, D. S., *Anal. Chem.*, 1979, **51,** 2364.
2 Slavin, W., Carnrick, G. R., and Manning, D. C., *Anal. Chem.*, 1984, **56,** 163.
3 Welz, B., Akman, S., and Schlemmer, G., *J. Anal. At. Spectrom.*, 1987, **2,** 793.
4 Churella, D. J., and Copeland, T. R., *Anal. Chem.*, 1978, **50,** 309.
5 Holcombe, J. A., Rayson, G. D., and Akerlind, N., *Spectrochim. Acta, Part B*, 1982, **37,** 319.
6 L'vov, B. V., *Spectrochim. Acta, Part B*, 1978, **33,** 153.
7 Frech, W., Persson, J. A., and Cedergren, A., *Prog. Anal. At. Spectrosc.*, 1980, **3,** 279.
8 Frech, W., and Cedergren, A., *Anal. Chim. Acta*, 1976, **82,** 83.
9 Cabon, J. Y., and Le Bihan, A., *Anal. Chim. Acta*, 1987, **198,** 87.
10 Hageman, L., Mubarak, A., and Woodriff, R., *Appl. Spectrosc.*, 1979, **33,** 226.
11 Ni, Z., Han, H, and Li, X., *J. Anal. At. Spectrom.*, 1986, **1,** 131.
12 Hulanicki, A., Bulska, E., and Dittrich, K., *J. Anal. At. Spectrom.*, 1990, **5,** 209.
13 McArthur, J. M., *Anal. Chim. Acta*, 1977, **93,** 77.
14 Carnrick, G. R., Slavin, W., and Manning, D. C., *Anal. Chem.*, 1981, **53,** 1866.
15 Pruszkowska, E., Carnrick, G. R., and Slavin, W., *Anal. Chem.*, 1983, **55,** 182.
16 Tominaga, M., and Umezaki, T., *Anal. Chim. Acta*, 1982, **139,** 279.
17 Hydes, D. J., *Anal. Chem.*, 1980, **52,** 959.
18 Regan, J. G. T., and Warren, J., *Analyst*, 1978, **103,** 447.
19 Gilchrist, G. F. R., Chakrabarti, C. L., and Byrne, J. P., *J. Anal. At. Spectrom.*, 1989, **4,** 533.
20 Gilchrist, G. F. R., Chakrabarti, C. L., Byrne, J. P., and Lamoureux, M., *J. Anal. At. Spectrom.*, 1990, **5,** 175.
21 Pingxin, W., and Tiezheng, L., *Spectrochim. Acta, Part B*, 1986, **41,** 1225.
22 Sturgeon, R. E., and Falk, H., *J. Anal. At. Spectrom.*, 1988, **3,** 27.
23 Frech, W., and Jonsson, S., *Spectrochim. Acta, Part B*, 1982, **37,** 1021.
24 Chakrabarti, C. L., in *Analytical Chemistry in the Exploration, Mining and Processing of Materials*, ed. Butler, L. R. P., Blackwell, Oxford, 1986, pp. 57–62.
25 Park, C. J., Van Loon, J. C., Arrowsmith, J., and French, J. B., *Can. J. Spectosc.*, 1987, **32,** 29.
26 Park, C. J., and Hall, G. E. M., *J. Anal. At. Spectrom.*, 1987, **2,** 473.
27 Sturgeon, R. E., Chakrabarti, C. L., and Langford, C. H., *Anal. Chem.*, 1976, **48,** 1792.
28 Erspamer, J. P., and Niemczyk, T. M., *Anal. Chem.*, 1982, **54,** 2150.
29 Welz, B., Akman, S., and Schlemmer, G., *Analyst*, 1985, **110,** 459.
30 Kántor, T., Bezúr, L., Pungor, E., and Winefordner, J. D., *Spectrochim. Acta, Part B*, 1983, **38,** 581.
31 Kántor, T., and Bezúr, L., *J. Anal. At. Spectrom.*, 1986, **1,** 9.
32 Fassel, V. A., *Pure Appl. Chem.*, 1977, **49,** 1533.

Paper 1/04312I
Received August 19, 1991
Accepted January 23, 1992